Article:

De Marco, M., Duzzi, D., Meneghello, F. et al. (1 more author) (2017) Cognitive Efficiency in Alzheimer's Disease is Associated with Increased Occipital Connectivity. Journal of Alzheimer's Disease, 57 (2). pp. 541-556. ISSN 1387-2877

https://doi.org/10.3233/JAD-161164

Cognitive Efficiency in Alzheimer's Disease is Associated with Increased Occipital Connectivity

Matteo De Marco[a,b], Davide Duzzi[b], Francesca Meneghello[b], Annalena Venneri[a,b]

[a]Department of Neuroscience, University of Sheffield, Royal Hallamshire Hospital, Beech Hill Road, S10 2RX, Sheffield, UK

[b]IRCCS Fondazione Ospedale San Camillo, Via Alberoni 70, 30126, Venice Lido, Italy

Running title

The network signature of efficiency in AD

Corresponding author

Prof. Annalena Venneri, Department of Neuroscience - Medical School, University of Sheffield, Beech Hill Road, Royal Hallamshire Hospital, N floor, room N130, Sheffield - S10 2RX - United Kingdom, a.venneri@sheffield.ac.uk, Tel: +44 114 2713430, Fax: +44 114 2222290

Abstract

There are cognitive domains which remain fully functional in a proportion of Alzheimer's disease (AD) patients. It is unknown, however, what distinctive mechanisms sustain such efficient processing. The concept of "cognitive efficiency" was investigated in these patients by operationalizing it as a function of the level of performance shown on the Letter Fluency test, on which, very often, patients in the early stages of AD show unimpaired performance.

Forty-five individuals at the prodromal/early stage of AD (diagnosis supported by subsequent clinical follow-ups) and 45 healthy controls completed a battery of neuropsychological tests and an MRI protocol which included resting-state acquisitions. The Letter Fluency test was the only task on which no between-group difference in performance was found. Participants were divided into "low-performing" and "high-performing" according to the global median. Dual-regression methods were implemented to compute six patterns of network connectivity. The diagnosis-by-level of performance interaction was inferred on each pattern to determine the network distinctiveness of efficient performance in AD.

Significant interactions were found in the anterior Default-Mode Network, and in both left and right Executive-Control Networks. For all three circuits, high-performing patients showed increased connectivity within the ventral and dorsal part of BA19, as confirmed by post-hoc t tests.

Peristriate remapping is suggested to play a compensatory role. Since the occipital lobe is the neurophysiological source of long-range cortical connectivity, it is speculated that the physiological mechanisms of functional connectivity might sustain occipital functional remapping in early AD, particularly for those functions which are sustained by areas not excessively affected by the prodromal disease.

Keywords

Alzheimer Disease, Cuneus, Cognitive Function, Magnetic Resonance Imaging

Introduction

When neurodegeneration of the Alzheimer type (AD) affects the neural tissue, it does not encounter a stable and otherwise unmodifiable environment. On the contrary, the mechanisms triggered by the pathology will concur and interact with the multidimensional non-pathological mechanisms of senescence. These processes of cerebral ageing entail a linear decrease of global volumetric properties of the neocortex [1] and, alongside this global linearity, a number of regions show age-dependent steeper non-linear, curve-shaped decrements [2]. In the context of such declining "hardware", the aging functional architecture of the brain circuitry undergoes processes of remapping which vary quantitatively and qualitatively network-by-network [3] and result in profound reshaping of connectivity patterns [4]. Inevitably, a large number of cognitive modules are, in turn, influenced by such modifications [5]. In fact, elderly adults tend to perform worse than young adults in a large number of tasks based on functions such as, for instance, episodic memory and executive control [6]. This description captures the central tendency of the progression along the aging time-line, but the scenario is necessarily accompanied by a degree of longitudinal dispersion, which results in individual-specific trajectories of aging, and which will also impact on the phenotype associated with the eventual onset of AD. This variability is heavily influenced by reserve processes [7], and by neurocognitive mechanisms responsible for efficiency, plasticity and compensation [8]. Within this set of mutually-associated notions, the concept of neural efficiency has been extensively investigated in healthy adulthood, in association with paradigms of intelligence and cognitive functioning [9]. In its original formulation, this concept refers to the mechanisms by which an optimal minimization of neuro-computational resources is associated with a maximization of task performance [10, 11]. Based on a considerable number of subsequent studies, the neural-efficiency hypothesis has then been re-arranged as a function of a number of modulatory variables which can influence the "less activation-better performance" mechanism, such as the level of task complexity, inter-individual differences in task expertise or task learning status, gender, type of cognitive functions under examination, and the topography of the computational areas involved in the task [9]. Evidence of diverse nature and diverse theoretical interpretation (i.e., the two somehow antithetic mechanisms of compensation and dedifferentiation) has shown that the efficient processing shown by elderly adults is strongly associated with the pattern of coactivation and connectivity of areas responsible for task computation [12-15]. An implementation of efficiency based on the concurrent recruitment of multiple areas is also directly implied by the studies which have investigated efficiency as a result of the modulation by anatomical connectivity in terms of white-matter integrity [16, 17]. Along a similar time-line, tightly concatenated with that of senescence, AD is associated with significant dysregulation of functional connectivity [18] and cognitive function, even at its prodromal stages [19]. The role of neural efficiency in AD, however, has been a largely unexplored research territory. A number of studies have investigated the association between declining functional connectivity of brain networks and residual cognitive performance [20, 21, 22]. These studies have shed some light on the relationship between functional reorganization of brain networks and cognitive performance in early degeneration, but they are not informative on the processes by which the neural system pursues efficiency. Reasonably, all brains in the early stages of AD are, to some extent, inefficient. Not all cognitive functions, however, are homogeneously affected by objective impairment. Within the set of cognitive tests administered to patients at increased risk of developing dementia of the AD type as part of clinical routine, performance on the Letter Fluency test is very often not primarily affected by the pathology. In fact, there are studies which have reported no differences in performance on this test between patients diagnosed with amnestic mild cognitive impairment and healthy adults [23-26], and between future converters and nonconverters to AD dementia [27]. Moreover, the mean annual change in the performance on this test is minimal for mild-cognitive-impairment patients subsequently converting to dementia of the AD type [28]. In addition, even patients diagnosed with fully-established AD very often show non-pathological performance on this test [29-31]. This test taps linguistic and executive processes [32], and its neural correlates are mainly located in left prefrontal areas [33, 34]. Since the performance on the Letter Fluency test is overall only minimally affected and often spared in the earliest stages of AD, it represents the best candidate to test a paradigm of neural efficiency. In this study we investigated the network-connectivity correlates of efficient performance on the Letter Fluency test in patients suffering from early AD. Specifically, we were interested in clarifying the distinct pattern of network connectivity associated with a performance not only within normal limits, but undistinguishable from that of high-performing healthy adults. To do so, we modelled the diagnosis-by-level of performance interaction, and we focused on six networks (Fig. 1). These were the posterior and anterior components of the default-mode network (pDMN - aDMN), the cerebellar network (CBN), and the left and right fronto-parietal executive-control network (lECN - rECN, respectively). The default-mode network was chosen based on its well-established association with cognitive performance, e.g., [35, 36]. The CBN was included based on the association between cerebellar sub-regions, semantic-processing and letter-fluency performance [37, 38]. Finally, parieto-frontal networks were selected because of their online role in executive control during task performance [39]. The occipital visual network (OVN) was additionally selected as methodological control, since it was expected not to play any crucial role in language and executive processing.

- Insert Fig. 1 about here -

Materials and Methods

Participants

In total, ninety participants were included in this study. Forty-five elderly adults experiencing and showing objective cognitive impairment of probable neurodegenerative nature were identified as part of their neurological assessment which followed a clinical referral to the outpatient clinic for memory disorders at the IRCCS Fondazione Ospedale San Camillo , Venice, Italy. Clinical effort was made to ascertain that all patients did not have aetiologies incompatible with AD. The recruitment of this sample had the objective of covering the continuum of early Alzheimer neurodegeneration spanning from a diagnosis of very mild dementia of probable Alzheimer aetiology [40] (n = 7) to a diagnosis of Mild Cognitive Impairment [41] suggestive of Alzheimer disease [42] (n = 38). In order to maximize the representativeness of the sample of the population of individuals suffering from Alzheimer's disease, patients with mild cognitive impairment were similarly included if they were of the amnestic or non-amnestic type. Both sub-types, in fact, can equally convert to dementia of the Alzheimer type [43], and serial clinical follow-ups from 2012 to 2016 confirmed the suspected aetiology of those cases which were initially uncertain. The sample included 7 amnestic single domain, 18 amnestic multiple domain, 10 non-amnestic single domain, and 3 non-amnestic multiple domain patients.

Forty-five healthy elderly adults were also included in the study. This sub-group matched the group of patients as closely as possible for age, levels of education, and gender ratio.

Exclusion criteria were set as follows: significant pharmacological treatments with psychotropic medications, drugs regulating cholinergic neurotransmission, drugs for research purposes or with toxic effects to internal organs, a clinically significant disease other than those consistent with the objective of the study, a baseline structural MRI revealing a major diagnostic entity not consistent with our study, presence/diagnosis of uncontrolled seizures, peptic ulcer, sick sinus syndrome, neuropathy with conduction difficulties, significant disabilities, evidence of abnormal baseline levels of folates, vitamin B12 or thyroid stimulating hormone, significant depression/anxiety or other psychiatric conditions.

Given the strong interplay which exists between cardiovascular mechanisms and Alzheimer's disease pathology [44-46], particular care was paid to assess the amount of vascular burden (i.e., white matter hyperintensity load) in patients and controls. Evidence of stroke or neural infarctions, or a history of transient ischemic attacks represented exclusion criteria, whereas amounts of hyperintensities normally judged by neuroradiologists as within normality for the age of each participant were reputed acceptable.

Diagnostic status was determined by a consensus among expert clinicians, and were based on cognitive levels, structural MRI evidence, a series of further clinical information including a neurological screening, scales measuring activities of daily living, and, most importantly, follow up examinations. These served as confirmatory support consistent with the neurodegenerative aetiology causing the cognitive impairment. Cognitive performance was determined based on an extensive battery of neuropsychological tests administered to each of the ninety participants by a senior neuropsychologist. Raw scores (reported in Table 1) and scores corrected for demographic characteristics served for a detailed delineation of the sample.

- Insert Table 1 about here -

All procedures were in accordance with the ethical standards of the institutional research committee and with the 1964 Helsinki declaration and its later amendments or comparable ethical standards. This study was approved by the Institutional Review Board of the IRCCS Fondazione Ospedale San Camillo (Venice, Italy), (Protocol N. 11/09 version 2). Informed consent was obtained from all individual participants included in the study.

MRI acquisition, processing, and modeling

All participants underwent an MRI (1.5 T, Philips Achieva) scanning protocol including anatomical sequences (T1 weighted, T2 weighted, FLAIR, these two latter modalities served to rule out exclusion criteria), and resting-state functional acquisitions.

Two runs (one hundred and twenty volumes each) of resting-state T2* images were recorded. Each image consisted of twenty axial slices acquired continuously with no gap. The following parameters were used: repetition time 2 s, echo delay time 50 ms, flip angle 90°, voxel dimensions 3.28 × 3.28 × 6.00 mm, field of view 230 mm. Each acquisition was preceded by twenty seconds of preliminary dummy scans, set to allow the scanner to reach equilibrium.

Turbo Field Echo 3D T1 weighted images were acquired for the analysis of brain structure. The following parameters were used: repetition time 7.4 ms, echo delay time 3.4 ms; flip angle 8°, voxel dimension 1.10 × 1.10 × 0.60 mm; field of view 250 mm; matrix size 256 × 256 × 124.

All participants were instructed to lay supine with eyes closed without falling asleep for the whole duration of the scan. Structural images were visually inspected by a senior neuroradiologist to safeguard compliance with the inclusion criteria and rejection of exclusion criteria. Images were analyzed with Statistical Parametric Mapping (SPM) 8, running in a Matlab R2011b (Mathworks Inc., UK) environment.

Aside from their clinical contribution, T1 weighted structural images were also processed for experimental purposes. A procedure based on standard Voxel-Based Morphology methodology was implemented [47]. This included probabilistic tissue-class (gray matter, white matter, and cerebrospinal fluid) segmentation in the Montreal Neurological Institute template-based 3D space, and a spatial smoothing carried out with an 8 mm^3 full-width at half maximum gaussian kernel. Additionally, tissue-class maps in the subject-specific native space were quantified using the "get_totals" Matlab function, and absolute and relative (fractional) indices of gray and white matter were calculated.

Resting-state functional MRI sequences were preprocessed and modeled using an in-house routine based on the sequential use of multiple toolboxes available in SPM 8. Scans were initially slice-timed and realigned in order to correct for intra-volume temporal displacement and inter-volume spatial dislocation. Plots of linear and rotational indices of in-scanner motion were visually inspected in order to rule out the presence of major artefacts. Similar to previously published research, e.g., [48-50], a threshold of 3 mm or 1.5 degrees was chosen as limit of acceptable in-scanner motion. Four participants showed movements exceeding these thresholds, and a volume-reduction was carried out to remove problematic images from the scan. In all cases the problematic images were removed either from the beginning or from the last portion of the scan not to disrupt the temporal dynamics of spontaneous BOLD fluctuations of neural origin [51], and preprocessing was restarted. By doing so, at least one hundred and eighty volumes were included in the analysis for each participant. Realigned images were then normalized in the Montreal Neurological Institute space using the echoplanar template available in SPM, and voxel size was isotropied to a 2 mm^3 cube. Consistent with our previous research [49], the REST toolbox [52] was used to band-passfilter at 0.008 hz - 0.01 hz the normalized images, which were subsequently smoothed with a 6 mm^3 full-width at half maximum gaussian kernel.

After preprocessing, patterns of network connectivity were computed based on a dual-regression procedure [53]. This method is based on (a) selecting maps of interest obtained via an Independent Component Analysis as topography from which to extract the MRI signal of individual datasets, and (b), using the resulting time-courses to compute individual spatial map (Fig. 1). This methodology had originally been designed to benefit from the inferential properties of both hypotheses-free latent-variable models and individual time-courses characterizing region-of-interest-based approaches. Briefly, the two runs of each participant were merged as one, and the Gift toolbox (v1.3i; mialab.mrn.org/software/gift) was used to run an Independent Component Analysis on the entire sample. This included a principal component analysis set to shortlist the sources of variability, the actual analysis based on the Infomax algorithm, and a GICA back reconstruction normally aimed at estimating participant-specific spatial maps and time-courses [54]. The number of components was set at 20, as carried out in previous landmark research [55]. The resulting z-score maps were visually inspected by two raters independently, who, in mutual agreement, selected the components which were spatially consistent with the networks of interest (Fig 1). The mean maps of these six components were binarized, and subject-specific time-courses were extracted from each seed using the MarsBaR toolbox [56]. Time-courses were also extracted from the normalized maps of white matter and cerebrospinal fluid resulting from the segmentation of the 3D T1 weighted anatomic template available in SPM. Individual maps of network connectivity were then calculated by regressing out in-scanner motion parameters and the average signal of white-matter and cerebrospinal-fluid maps. Following this procedural pipeline, t-test models were run to characterize diagnosis-dependent differences between the two sub-groups.

Performance on the Letter Fluency test was not correlated with Mini Mental State Examination scores neither in the sub-group of healthy adults (*Spearman's rho* = 0.270; p = 0.072) nor in the sub-group of patients (*Spearman's rho* = 0.242; p = 0.110), and this was the only task for which no between-group difference was observed either in the analysis of raw uncorrected scores or in that of scores corrected for age and education level, as determined by the Italian normative data published in a number of studies [57-63]. The median score was calculated for the raw score obtained on this test (= 31 words), and the entire group was split in two halves according to this value. This generated four sub-groups (low-performance healthy controls, high-performance healthy controls, low-performance patients, high-performance patients). Demographic, neuropsychological, and global neurostructural characteristics of the four sub-groups are reported in Table 2.

- Insert Table 2 about here –

The interaction between diagnostic status and level of Letter-Fluency performance was then modelled. Additional variables were included in the interaction models as nuisance regressors. These included age, total intracranial volume as a proxy of brain reserve [64], and education levels as a proxy of cognitive reserve [65]. Whenever an interaction yielded significant findings, these were further explored with post hoc t-test models, comparing low-performing and high-performing adults within each diagnostic group. The set-level threshold of significance was set for all analyses at an uncorrected $p < 0.001$ to account for 6 multiple comparisons (Bonferroni-corrected $p < 0.01$). Model-specific minimum cluster size was defined as the $p < 0.05$ threshold resulting from AlphaSim simulations (http://afni.nimh.nih.gov/afni/) based on conservative parallelepipedal matrices containing a number of voxels larger than that of the voxels analyzed in the models, a cluster connection radius = 2.5 mm, axial gaussian filters as indicated in the SPM output, and 5000 repetitions. Output coordinates were converted from Montreal National Institute to Talairach space by means of a nonlinear transformation (http://imaging.mrc-cbu.cam.ac.uk/downloads/MNI2tal/mni2tal-m). The Talairach Daemon Client [66] was then used for interpretation purposes ("Nearest Gray Matter" search option).

Results

Substantial and widespread volumetric differences were found between the two diagnostic groups, with patients having smaller gray-matter volumes in a large number of cortical and subcortical regions, bilaterally, and extending to all lobes. With a focus on brain networks, the sub-group of healthy controls had more functional connectivity than the sub-group of patients: 1) within the pDMN, in a cluster including middle- and posterior cingulate regions, and 2) within the OVN, in the caudate nucleus. Significant differences in the opposite direction were found 3) within the CBN, with increased connectivity seen in patients in motor/premotor areas, and 4) within the rECN, with increased connectivity observed in the left superior parietal cortex. No group difference was found in the pattern of functional connectivity within the lECN or aDMN. All group differences are illustrated in Table 3

- Insert Table 3 about here -

Significant group-by-level of performance interactions were found in three out of six patterns of network connectivity. The contrast of interest yielded significant clusters within the lECN, the rECN and the aDMN (Table 4; Fig. 2).

- Insert Table 4 and Fig. 2 about here –

Within the lECN, a significant effect of the interaction was found in precuneal/cuneal regions and in the posterior portion of the middle temporal gyrus. Post hoc testing indicated high performing patients had more connectivity within these areas than low-performing patients, whereas no difference was found in the control sub-groups (Table 5). Within the rECN, a significant effect of the interaction was found in a midline cluster located between the cuneus and the posterior cingulate. Post hoc testing indicated high-performing patients had more connectivity within these areas than low-performing patients, and, in addition, they also had increased connectivity in left temporal regions (Table 5). Again, no difference was found in the control sub-groups. Within the aDMN, a significant effect of the interaction was found in cuneal and precuneal territory. The post hoc comparisons revealed no between-group difference in the sub-groups of healthy adults, whereas high-performing patients showed increased functional connectivity in the temporo-occipital extrastriate regions (Table 5). The opposite contrast yielded no significant interaction.

- Insert Table 5 about here -

No structural differences were found between high-performing and low-performing participants. This was the case for both diagnostic sub-groups.

To understand whether the interaction term was driven by low-performing patients having significantly lower functional connectivity than controls or high-performing patients having significantly higher functional connectivity than controls, a further post-hoc analysis was carried out. Subject-specific statistical indices of connectivity were extracted from the four clusters where a significant interaction had been found (each cluster in association with its specific map of connectivity). These were then analyzed with SPSS with 1×4 ANOVAs to compare the four sub-groups, and, since Bonferroni-corrected t tests revealed no differences in connectivity between high-performing and low-performing controls, these were collapsed in a single group. A 1×3 ANOVA was then run, and Bonferroni-corrected t tests revealed that the interaction was driven by low-performing patients having significantly less connectivity than controls in the aDMN and rECN clusters, and by high-performing patients having significantly more connectivity than controls in the two lECN clusters (Fig. 3)

- Insert Fig. 3 about here -

Discussion

We investigated the network correlates of efficient task-performance in early neurodegeneration for the Letter Fluency test, for which patients in the early stages of AD very often show unimpaired performance. This choice was made to understand what distinct patterns of network connectivity are associated with efficient performance, where "efficient" does not simply mean within normal limits, but refers to a score above the median value pooled from a group including healthy controls.

Efficiency and extrastriate connectivity

The first, quantitative finding is that, in AD, efficiency is not warranted through optimization of neural resources, as originally formulated [10, 11], but rather in association with an increase in the magnitude of network connectivity. This is in contrast with decreases in task co-activation and connectivity detected in efficient young adults [12, 14, 67, 68], and in line with the increase described in elderly adulthood [69]. It is also consistent with the model of hemispheric asymmetry reduction, in which high-level performance is sustained by increased bilateral co-activation [70, 71], and with evidence from the study of functional connectivity [13]. Although there is evidence that patients with mild cognitive impairment often show increased activation of areas of primary relevance for the task of reference, often as an effect of compensatory mechanisms [72], we hereby find evidence indicating that a highly efficient cognitive performance in early AD is found in concomitance with widespread alterations of functional connectivity. Structural analyses ruled out the possibility that volumetric differences could be crucially involved in this mechanism. The second, qualitative finding emerging from this study is that network connectivity of occipital and, to a lesser extent, temporo-parietal regions is associated with cognitive efficiency in early neurodegeneration. Particularly, the cuneus emerged as an area of primary importance, contributing to three separate patterns of functional connectivity.

The extrastriate territory is significantly affected by neurofibrillary pathology during the limbic stage of clinical AD [73], and hypoperfusion of the cuneus is also observed in mild cognitive impairment of the amnestic type [74], suggesting a potential pathological down-regulation of this territory in prodromal AD. Occipital hypermetabolism is instead detectable in amnestic mild cognitive impairment free from amyloid burden, and thus not suggestive of AD [75]. Being the occipital lobe a territory characterized by relatively healthy neural tissue, it is possible that this region might offer connectivity support to those functions (e.g., letter fluency abilities) which normally rely on other areas not dramatically affected by the disease, and thus prone to plastic remodeling.

Connectivity as a framework to study efficiency

Although neurocognitive efficiency, traditionally, has been studied as a function of signal change in task-related functional MRI, we investigated resting-state networks. This choice was made for multiple reasons. First, it is well-established that brain networks responsible for the engagement in a cognitive task are the same as those "dynamically active" during resting-state [76]. Second, the study of resting-state networks is particularly informative about the characterization of neural disruption seen in neurodegenerative patients [77]. Third, this methodological choice facilitates inter-study comparisons (e.g., see [78] for an example of how much variability is found when multiple task-related paradigms are similar but not identical). Fourth, different task-based activations might also be due to differences in the computational strategies implemented to perform the target operation [72]. Choosing a paradigm based on resting state minimizes this risk. Fifth, the pattern of connectivity represents a hierarchical organization of brain function which is more high-level than the pattern of task-related activation. In fact, the connectivity statistic yielded by each voxel represents the "interaction" between two neural sources, and this supersedes the "main effects" seen in each of these neural sources during activation paradigms.

The role of occipital function in neural synchronicity

Evidence in support of functional down-regulation of the cuneus in early AD is also provided by studies which have explored the physiology of the occipital lobe. This qualitatively different approach of investigating cortical functioning is informative in this context because "synchronization of neural assemblies is a process that spans multiple spatial and temporal scales in the nervous system" [79, page 231]. It is well-established that the occipital lobe is the cortical region where alpha rhythms are particular prominent at rest, when eyes are closed [80]. Resting-state occipital alpha rhythms are positively associated with gray-matter density and cognitive functioning in early AD [81], and, specifically, the functional network disruption typically seen in the DMN of amnestic mild cognitive impairment patients occurs within the alpha rhythms [82].

Oscillations within the alpha frequency band are believed to subserve long-range connectivity circuits [12, 83], and it has been suggested they influence both "task positive" and "task negative" haemodynamic patterns [84, 85, 86]. Although it is not possible to interpret our findings as a function of a neurophysiological causative mechanism, the body of evidence we collected indicates that peristriate regions located within the neurophysiological core of long-range cortical brain networks, and showing functional modifications in the early clinical stages leading to AD dementia, are the regions in which haemodynamics differ between efficient and non-efficient patients with early-stage neurodegenerative disruption. This might translate into a future testable hypothesis.

It is possible that the involvement of the extrastriate complex is the result of compensatory mechanisms. In a recent study functional connectivity between prefrontal and occipital regions was interpreted as compensatory for task-switching in elderly adults [13]. A hypothesis of occipital compensation in AD is supported by our post-hoc findings. These revealed that the statistical role of the peristriate clusters was driven by high-performing patients, who differently from low-performing patients, either retained levels of connectivity comparable to those of controls, or showed significantly more connectivity than controls. Based on this, we speculate that high performance in early-stage AD might be supported by optimal levels of network connectivity within the occipital lobe, or by compensatory up-regulation, or by an interplay of both. It remains to be determined (a) why some patients benefit from these forms of compensation, whereas others do not, and (b) why certain brain networks contribute to cognitive efficiency, while others do not. Importantly, although the occipital lobe is deeply involved in visual processing, no significant interaction effect was found within the connectivity of the OVN. This suggests that the differences found in occipital connectivity may reflect a high-order and not a sensory computational processing.

Alongside the cuneal involvement, significant effects of the interaction in other areas (the precuneus and Brodmann Area 30-31) were not confirmed by post-hoc comparisons. These highlighted instead the role of the cuneus and the portion of the left temporo-occipital junction located in Brodmann Area 19. Differences in the latter, in particular, were found in all post hoc voxel-by-voxel comparisons between high-performing and low-performing patients. Even though the territory of the left temporo-occipital junction is associated with high order processing of complex visual stimuli [86], its involvement in support of resting-state brain networks suggests that it might also serve a compensatory function in early neurodegeneration, in a fashion similar to the more ventral portions of Brodmann Area 19 as discussed above, or to prefrontal regions, which are up-regulated in the DMN of patients with mild cognitive impairment [87, 88]. It is important to highlight that the differences in efficiency between the two sub-groups of patients cannot be significantly ascribed to different levels of brain reserve or cognitive reserve, as shown by non-significant group-differences on measured variables associated with these concepts (Table 2). Moreover, proxies of brain and cognitive reserve were included in all models as nuisance regressors. Another speculation to rule out is the possibility that low-performing patients simply were at a more advanced level of neural disruption. We challenge this explanation because no difference other than that in letter fluency was found between the two sub-groups for any of the tests of memory, visuospatial skills or language, nor on the Mini Mental State Examination (Table 2). This indicates that the separation of low- and high-performers did not reflect a difference in the general level of cognitive decline or disease severity.

Potential limitations

The main weakness associated with this study is the theoretical discrepancy between our operationalization of efficiency and that so far utilized in research. When brain function is unimpaired, it is relatively straightforward to interpret the performance/activation (or performance/connectivity) ratio as a measure of efficiency. On the other hand, it is more complicated to explore this same construct in groups of brains which have been rendered inefficient by neurodegeneration. Second, although we separated the group of patients into two sub-group according to the scores obtained on a single neuropsychological test, all patients were, in a global sense, “low-performing”. We argue that efficiency in very mild neurodegeneration can only be explored in association with single tasks, which do not reflect the general level of retained competence, but are instead representative of a cognitive aspect not primarily affected by the diagnostic entity. An alternative approach would consist of investigating the pattern of activation in patients and controls using a simple task in which both groups would generally show good performance, e.g., [89]. This latter choice, however, would generate limited variability in behavioral measures among healthy controls. A third weakness is the level of complexity of the task. Even though the study of neurocognitive efficiency has been mostly carried out in association with paradigms of working memory or speed of processing, there are paradigms which have explored this hypothesis in association with tasks which do not show a heavy load on these basic executive functions (see [9] for a review). In addition, there has been a preferential use of isolated cognitive operations rather than multi-componential cognitive tasks [68]. We acknowledge that letter fluency is influenced by an interaction of verbal and executive processes [32] and it might be thus difficult to disentangle the nature of the neural optimization which leads to efficient processing. Nevertheless, we chose this test following a pragmatic approach since it reflects a measure which has diagnostic properties, it is used in clinical settings, and it is associated with a well-established literature and frame of reference.

In conclusion, our findings indicate that neurocognitive efficiency in verbal-executive skills in early AD is associated with increased network connectivity within extrastriate regions, likely as a result of compensatory mechanisms.

Acknowledgements

We would like to thank Cristina Pilosio, Jessica Rigon, and Francesca Burgio for their precious contribution to cognitive data collection. We would also like to thank Francesco Spigariol, Luciano Foscolo, Valentina Citton, Luca Ghezzo, Elisa Duse and Antonio Tumbarello for helping with MRI data collection. The authors declare no conflict of interest.

This study was funded by grant No 42/RF-2010-2321718 by the Italian Ministry of Health to AV and from partial funding from the European Union Seventh Framework Programme (FP7/2007 – 2013) under grant agreement no. 601055, VPH-DARE@IT to AV.

References

[1] Ge YL, Grossman RI, Babb JS, Rabin ML, Mannon LJ, Kolson DL (2002) Age-related total gray matter changes in normal adult brain. Part I: Volumetric MR imaging analysis. AJNR Am J Neuroradiol **23**, 1327-1333.

[2] Ziegler G, Dahnke R, Jäncke L, Yotter RA, May A, Gaser C (2012) Brain structural trajectories over the adult lifespan. Hum Brain Mapp **33**, 2377-2389.

[3] Mowinckel AM, Espeseth T, Westlye LT (2012) Network-specific effects of age and in-scanner subject motion: A resting-state fMRI study of 238 healthy adults. Neuroimage **63**, 1364-1373.

[4] Liu ZL, Ke LN, Liu HF, Huang WH, Hu ZH (2014) Changes in topological organization of functional PET brain network with normal aging. PLoS One **9**, e88690.

[5] Samson RD, Barnes CA (2013) Impact of aging brain circuits on cognition. Eur J Neurosci **37**, 1903-1915.

[6] Deary IJ, Corley J, Gow AJ, Harris SE, Houlihan LM, Marioni RE, Penke L, Rafnsson SB, Starr JM (2009) Age-associated cognitive decline. Br Med Bull **92**, 135-152.

[7] Stern Y (2009) Cognitive reserve. Neuropsychologia **17**, 2015-2028.

[8] Barulli D, Stern Y (2013) Efficiency, capacity, compensation, maintenance, plasticity: Emerging concepts in cognitive reserve. Trends Cogn Sci **17**, 502-509.

[9] Neubauer AC, Fink A (2009) Intelligence and neural efficiency. Neurosci Biobehav Rev **33**, 1004-1023.

[10] Haier RJ, Siegel BV Jr, Nuechterlein KH, Hazlett E, Wu JC, Paek J, Browning HL, Buchsbaum MS (1988) Cortical glucose metabolic rate correlates of abstract reasoning and attention studied with positron emission tomography. Intelligence **12**, 199-217.

[11] Haier RJ, Siegel BV Jr, MacLachlan A, Soderling E, Lottenberg S, Buchsbaum MS (1992) Regional glucose metabolic changes after learning a complex visuospatial/motor task: a positron emission tomographic study. Brain Res **570**, 134-143.

[12] del Río D, Cuesta P, Bajo R, García-Pacios J, López-Higes R, del-Pozo F, Maestú F (2012) Efficiency at rest: magnetoencephalographic resting-state connectivity and individual differences in verbal working memory. Int J Psychophysiol **86**, 160-167.

[13] Hakun JG, Zhu Z, Johnson NF, Gold BT (2015) Evidence for reduced efficiency and successful compensation in older adults during task switching. Cortex **64**, 352-362.

[14] Rypma B, Berger JS, Prabhakaran V, Bly BM, Klimberg DY, Biswal BB, D'Esposito M (2006) Neural correlates of cognitive efficiency. Neuroimage **33**, 969-979.

[15] Vakhtin AA, Ryman SG, Flores RA, Jung RE (2014) Functional brain networks contributing to the Parieto-Frontal Integration Theory of Intelligence. Neuroimage **103**, 349-354.

[16] Burzynska AZ, Wong CN, Voss MW, Cooke GE, McAuley E, Kramer AF (2015) White matter integrity supports BOLD signal variability and cognitive performance in the aging human brain. PLoS One **10**, e0120315.

[17] Gao J, Cheung RT, Chan YS, Chu LW, Mak HK, Lee TM (2014) The relevance of short-range fibers to cognitive efficiency and brain activation in aging and dementia. PLoS One **9**, e90307.

[18] Song J, Qin W, Liu Y, Duan Y, Liu J, He X, Li K, Zhang X, Jiang T, Yu C (2013) Aberrant functional organization within and between resting-state networks in AD. PLoS One **8**, e63727.

[19] Weintraub S, Wicklund AH, Salmon DP (2012) The neuropsychological profile of Alzheimer disease. Cold Spring Harb Perspect Med **2**, a006171.

[20] Dunn CJ, Duffy SL, Hickie IB, Lagopulous J, Lewis SJ, Naismith SL, Shine JM (2014) Deficits in episodic memory retrieval reveal impaired default mode network connectivity in amnestic mild cognitive impairment. Neuroimage Clin **4**, 473-480.

[21] Gardini S, Venneri A, Sambataro F, Cuetos F, Fasano F, Marchi M, Crisi G, Caffarra P (2015) Increased functional connectivity in the default mode network in mild cognitive impairment: A maladaptive compensatory mechanism associated with poor semantic memory performance. J Alzheimers Dis **45**, 457-470.

[22] Yue C, Wu D, Bai F, Shi Y, Yu H, Xie C, Zhang Z (2015) State-based functional connectivity changes associate with cognitive decline in amnestic mild cognitive impairment subjects. Behav Brain Res **288**, 94-102.

[23] Libon DJ, Xie SX, Eppig J, Wicas G, Lamar M, Lippa C, Bettcher BM, Price CC, Giovannetti T, Swenson R, Wambach DM (2010) The heterogeneity of mild cognitive impairment: A neuropsychological analysis. J Int Neuropsychol Soc **16**, 84-93.

[24] Lonie JA, Herrmann LL, Tierney KM, Donaghey C, O'Carroll R, Lee A, Ebmeier KP (2009) Lexical and semantic fluency discrepancy scores in aMCI and early Alzheimer's disease. J Neuropsychol **3**, 79-92.

[25] Murphy KJ, Rich JB, Troyer AK (2006) Verbal fluency patterns in amnestic mild cognitive impairment are characteristic of Alzheimer's type dementia. J Int Neuropsychol Soc **12**, 570-574.

[26] Price SE, Kinsella GJ, Ong B, Mullaly E, Phillips M, Pangnadasa-Fox L, Perre D, Storey E (2010) Learning and memory in amnestic mild cognitive impairment: contribution of working memory. J Int Neuropsychol Soc **16**, 342-351.

[27] Gallagher D, Mhaolain AN, Coen R, Walsh C, Kilroy D, Belinski K, Bruce I, Coakley D, Walsh JB, Cunningham C, Lawlor BA (2010) Detecting prodromal Alzheimer's disease in mild cognitive impairment: utility of the CAMCOG and other neuropsychological predictors. Int J Geriatr Psychiatry **25**, 1280-1287.

[28] Mura T, Proust-Lima C, Jacqmin-Gadda H, Akbaraly TN, Touchon J, Dubois B, Berr C (2014) Measuring cognitive change in subjects with prodromal Alzheimer's disease. J Neurol Neurosurg Psychiatry **85**, 363-370.

[29] Bizzozero I, Scotti S, Clerici F, Pomati S, Laiacona M, Capitani E (2013) On which abilities are category fluency and letter fluency grounded? A confirmatory factor analysis of 53 Alzheimer's dementia patients. Dement Geriatr Cogn Dis Extra **3**, 179-191.

[30] Capitani E, Rosci C, Saetti MC, Laiacona M (2009) Mirror asymmetry of category and letter fluency in traumatic brain injury and Alzheimer's disease. Neuropsychologia **47**, 423-429.

[31] Herbert V, Brookes RL, Markus HS, Morris RG (2014) Verbal fluency in cerebral small vessel disease and Alzheimer's disease. J Int Neuropsychol Soc **20**, 413-421.

[32] Shao Z, Janse E, Visser K, Meyer AS (2014) What do verbal fluency tasks measure? Predictors of verbal fluency performance in older adults. Front Psychol **5**, 772.

[33] Biesbroek JM, van Zandvoort MJ, Kappelle LJ, Velthuis BK, Biessels GJ, Postma A (2015) Shared and distinct anatomical correlates of semantic and phonemic fluency revealed by lesion-symptom mapping in patients with ischemic stroke. Brain Struct Funct **221**, 2123-2134.

[34] Meinzer M, Flaisch T, Wilser L, Eulitz C, Rockstroh B, Conway T, Gonzalez-Rothi L, Crosson B (2009) Neural signatures of semantic and phonemic fluency in young and old adults. J Cogn Neurosci **21**, 2007-2018.

[35] Esposito F, Aragri A, Latorre V, Popolizio T, Scarabino T, Cirillo S, Marciano E, Tedeschi G, Di Salle F (2009) Does the default-mode functional connectivity of the brain correlate with working-memory performances? Arch Ita Biol **147**, 11-20.

[36] Yakushev I, Chételat G, Fischer FU, Landeau B, Bastin C, Scheurich A, Perrotin A, Bahri MA, Drzezga A, Eustache F, Schreckenberger M, Fellgiebel A, Salmon E (2013) Metabolic and structural connectivity within the default mode network relates to working memory performance in young healthy adults. Neuroimage **79**, 184-190.

[37] Arasanz CP, Staines R, Roy EA, Schweizer TA (2012) The cerebellum and its role in word generation: A cTBS study. Cortex **48**, 718-724.

[38] Venneri A, McGeown WJ, Hietanen HM, Guerrini C, Ellis AW, Shanks MF (2008) The anatomical bases of semantic retrieval deficits in early Alzheimer's disease. Neuropsychologia **46**, 497-510.

[39] Zanto TP, Gazzaley A (2013) Fronto-parietal network: flexible hub of cognitive control. Trends Cogn Sci 17, 602-603.

[40] Dubois B, Feldman HH, Jacova C, Hampel H, Molinuevo JL, Blennow K, DeKosky ST, Gauthier S, Selkoe D, Bateman R, Cappa S, Crutch S, Engelborghs S, Frisoni GB, Fox NC, Galasko D, Habert MO, Jicha GA, Nordberg A, Pasquier F, Rabinovici G, Robert P, Rowe C, Salloway S, Sarazin M, Epelbaum S, de Souza LC, Vellas B, Visser PJ, Schneider L, Stern Y, Scheltens P, Cummings JL (2014) Advancing research diagnostic criteria for Alzheimer's disease: the IWG-2 criteria. Lancet Neurol **13**, 614-629.

[41] Petersen RC (2004) Mild cognitive impairment as a diagnostic entity. J Int Med **256**, 183-194.

[42] Albert MS, DeKosky ST, Dickson D, Dubois B, Feldman HH, Fox NC, Gamst A, Holtzman DM, Jagust WJ, Petersen RC, Snyder PJ, Carrillo MC, Thies B, Phelps CH (2011) The diagnosis of mild cognitive impairment due to Alzheimer's disease: recommendations from the National Institute on Aging-Alzheimer's Association workgroups on diagnostic guidelines for Alzheimer's disease. Alzheimers Dement **7**, 270-279.

[43] Fischer P, Jungwirth S, Zehetmayer S, Weissgram S, Hoenigschnabl S, Gelpi E, Krampla W, Tragl KH (2007) Conversion from subtypes of mild cognitive impairment to Alzheimer dementia. Neurology **68**, 288-291.

[44] Di Marco LY, Farkas E, Martin C, Venneri A, Frangi AF (2015) Is vasomotion in cerebral arteries impaired in Alzheimer's disease? J Alzheimers Dis **46**, 35-53.

[45] Craft S (2009) The role of metabolic disorders in Alzheimer disease and vascular dementia: two roads converged. Arch Neurol **66**, 300-305.

[46] Schneider JA, Arvanitakis Z, Bang WJ, Bennett DA (2007) Mixed brain pathologies account for most dementia cases in community-dwelling older persons. Neurology **69**, 2197-2204.

[47] Ashburner J, Friston KJ (2000) Voxel-based morphometry--the methods. Neuroimage **11**, 805-821.

[48] Arenaza-Urquijo EM, Landeau B, La Joie R, Mevel K, Mézenge F, Perrotin A, Desgranges B, Bartrés-Faz D, Eustache F, Chételat G (2013) Relationships between years of education and gray matter volume, metabolism and functional connectivity in healthy elders. Neuroimage **83**, 450-457.

[49] De Marco M, Meneghello F, Duzzi D, Rigon J, Pilosio C, Venneri A (2016) Cognitive stimulation of the default-mode network modulates functional connectivity in healthy ageing. Brain Res Bull **121**, 26-41.

[50] Mevel K, Landeau B, Fouquet M, La Joie R, Villain N, Mézenge F, Perrotin A, Eustache F, Desgranges B, Chételat G (2013) Age effect on the default mode network, inner thoughts, and cognitive abilities. Neurobiol Aging **34**, 1292-1301.

[51] Fox MD, Raichle ME (2007) Spontaneous fluctuations in brain activity observed with functional magnetic resonance imaging. Nat Rev Neurosci **8**, 700-711.

[52] Song XW, Dong ZY, Long XY, Li SF, Zuo XN, Zhu CZ, He Y, Yan CG, Zang YF (2011) REST: A toolkit for resting-state functional magnetic resonance imaging data processing. PLoS One **6**, e25031.

[53] Filippini N, MacIntosh BJ, Hough MG, Goodwin GM, Frisoni GB, Smith SM, Matthews PM, Beckmann CF, Mackay CE (2009) Distinct patterns of brain activity in

young carriers of the APOE-epsilon4 allele. Proc Natl Acad Sci U S A **106**, 7209-7214.

[54] Calhoun VD, Adali T, Pearlson GD, Pekar JJ (2001) A method for making group inferences from functional MRI data using independent component analysis. Hum Brain Mapp **14**, 140-151.

[55] Biswal BB, Mennes M, Zuo XN, Gohel S, Kelly C, Smith SM, Beckmann CF, Adelstein JS, Buckner RL, Colcombe S, Dogonowski AM, Ernst M, Fair D, Hampson M, Hoptman MJ, Hyde JS, Kiviniemi VJ, Kötter R, Li SJ, Lin CP, Lowe MJ, Mackay C, Madden DJ, Madsen KH, Margulies DS, Mayberg HS, McMahon K, Monk CS, Mostofsky SH, Nagel BJ, Pekar JJ, Peltier SJ, Petersen SE, Riedl V, Rombouts SA, Rypma B, Schlaggar BL, Schmidt S, Seidler RD, Siegle GJ, Sorg C, Teng GJ, Veijola J, Villringer A, Walter M, Wang L, Weng XC, Whitfield-Gabrieli S, Williamson P, Windischberger C, Zang YF, Zhang HY, Castellanos FX, Milham MP (2010) Toward discovery science of human brain function. Proc Natl Acad Sci U S A **107**, 4734-4739.

[56] Brett M, Anton JL, Valabregue R, Poline JB (2002) Region of interest analysis using an SPM toolbox [abstract] Presented at the 8th International Conference of Functional Mapping of the Human Brain, June 2-6, 2002, Sendai, Japan. Neuroimage **16**(2).

[57] Basso A, Capitani E, Laiacona M (1987) Raven's coloured progressive matrices: normative values on 305 adult normal controls. Funct Neurol **2**, 189-194.

[58] Caffarra P, Vezzadini G, Dieci F, Zonato F, Venneri A (2002a) Una versione abbreviata del test di Stroop: dati normativi nella popolazione italiana. Nuova Rivista di Neurologia **12**, 111-115.

[59] Caffarra P, Vezzadini G, Dieci F, Zonato F, Venneri A (2002b) Rey-Osterrieth complex figure: normative values in an Italian population sample. Neurol Sci **22**, 443-447.

[60] Novelli A, Papagno C, Capitani E, Laiacona M, Cappa S, Vallar G (1986a) Tre test clinici di memoria verbale a lungo termine. Archivio di Psicologia, Neurologia e Psichiatria **47**, 278-296.

[61] Novelli G, Papagno C, Capitani E, Laiacona M, Vallar G, Cappa SF (1986b) Tre test clinici di ricerca e produzione lessicale. Taratura su soggetti normali. Archivio di Psicologia, Neurologia e Psichiatria **47**, 477-506.

[62] Orsini A, Grossi D, Capitani E, Laiacona M, Papagno C, Vallar G (1987) Verbal and spatial immediate memory span - normative data from 1355 adults and 1112 children. Ital J Neurol Sci **8**, 539-548.

[63] Spinnler H, Tognoni G (1987) Standardizzazione e taratura italiana di test neuropsicologici. Ital J Neurol Sci **6**, 1-120.

[64] Edland SD, Xu Y, Plevak M, O'Brien P, Tangalos EG, Petersen RC, Jack CR Jr (2002) Total intracranial volume: normative values and lack of association with Alzheimer's disease. Neurology **59**, 272-274.

[65] Liu Y, Cai ZL, Xue S, Zhou X, Wu F (2013) Proxies of cognitive reserve and their effects on neuropsychological performance in patients with mild cognitive impairment. J Clin Neurosci **20**, 548–553.

[66] Lancaster JL, Woldorff MG, Parsons LM, Liotti M, Freitas CS, Rainey L, Kochunov PV, Nickerson D, Mikiten SA, Fox PT (2000) Automated Talairach Atlas labels for functional brain mapping. Hum Brain Mapp **10**, 120-131.

[67] Majerus S, Belayachi S, De Smedt B, Leclercq AL, Martinez T, Schmidt C, Weekes B, Maquet P (2008) Neural networks for short-term memory for order differentiate high and low proficiency bilinguals. Neuroimage **42**, 1698-1713.

[68] Rao NK, Motes MA, Rypma B (2014) Investigating the neural bases for intra-subject cognitive efficiency changes using functional magnetic resonance imaging. Front Hum Neurosci **8**, 840.

[69] Motes MA, Biswal BB, Rypma B (2011) Age-dependent relationships between prefrontal cortex activation and processing efficiency. Cogn Neurosci **2**, 1-10.

[70] Cabeza R (2002) Hemispheric Asymmetry Reduction in Older Adults: The HAROLD model. Psychol Aging **17**, 85-100.

[71] Cabeza R, Anderson ND, Locantore JK, McIntosh AR (2002) Aging gracefully: compensatory brain activity in high-performing older adults. Neuroimage **17**, 1394-1402.

[72] Han SD, Bangen KJ, Bondie MW (2009) Functional magnetic resonance imaging of compensatory neural recruitment in aging and risk for Alzheimer's disease: Review and recommendations. Dement Geriatr Cogn Disord **27**, 1–10.

[73] Braak H, Braak E (1991) Neuropathological stageing of Alzheimer-related changes. Acta Neuropathol **82**, 239-259.

[74] Ding B, Ling HW, Zhang Y, Huang J, Zhang H, Wang T, Yan FH (2014) Pattern of cerebral hyperperfusion in Alzheimer's disease and amnestic mild cognitive impairment using voxel-based analysis of 3D arterial spin-labeling imaging: initial experience. Clin Interv Aging **9**, 493-500.

[75] Ashraf A, Fan Z, Brooks DJ, Edison P (2015) Cortical hypermetabolism in MCI subjects: a compensatory mechanism? Eur J Nucl Med Mol Imaging **42**, 447-458.

[76] Smith SM, Fox PT, Miller KL, Glahn DC, Fox PM, Mackay CE, Filippini N, Watkins KE, Toro R, Laird AR, Beckmann CF (2009) Correspondence of the brain's functional architecture during activation and rest. Proc Natl Acad Sci U S A **106**, 13040-13045.

[77] Seeley WW, Crawford RK, Zhou J, Miller BL, Greicius MD (2009) Neurodegenerative diseases target large-scale human brain networks. Neuron **62**, 42-52.

[78] Trachtenberg AJ, Filippini N, Mackay CE (2012) The effects of APOE-ε4 on the BOLD response. Neurobiol Aging **33**, 323-334.

[79] Varela F, Lachaux JP, Rodriguez E, Martinerie J (2001) The brainweb: phase synchronization and large-scale integration. Nat Rev Neurosci **2**, 229-239.

[80] Cohn R (1948) The occipital alpha rhythm; a study of phase variations. J Neurophysiol **11**, 31-37.

[81] Babiloni C, Del Percio C, Boccardi M, Lizio R, Lopez S, Carducci F, Marzano N, Soricelli A, Ferri R, Triggiani AI, Prestia A, Salinari S, Rasser PE, Basar E, Famà F, Nobili F, Yener G, Emek-Savaş DD, Gesualdo L, Mundi C, Thompson PM, Rossini PM, Frisoni GB (2015) Occipital sources of resting-state alpha rhythms are related to local gray matter density in subjects with amnesic mild cognitive impairment and Alzheimer's disease. Neurobiol Aging **36**, 556-570.

[82] Garcés P, Angel Pineda-Pardo J, Canuet L, Aurtenetxe S, López ME, Marcos A, Yus M, Llanero-Luque M, Del-Pozo F, Sancho M, Maestú F (2014) The Default Mode

Network is functionally and structurally disrupted in amnestic mild cognitive impairment - a bimodal MEG-DTI study. Neuroimage Clin **6**, 214-221.

[83] Palva S, Palva JM (2011) Functional roles of alpha-band phase synchronization in local and large-scale cortical networks. Front Psychol **2**, 204.

[84] Mayhew SD, Ostwald D, Porcaro C, Bagshaw AP (2013) Spontaneous EEG alpha oscillation interacts with positive and negative BOLD responses in the visual-auditory cortices and default-mode network. Neuroimage **76**, 362-372.

[85] Mo J, Liu Y, Huang H, Ding M (2013) Coupling between visual alpha oscillations and default mode activity. Neuroimage **68**, 112-118.

[86] Vogel AC, Petersen SE, Schlaggar BL (2012) The left occipitotemporal cortex does not show preferential activity for words. Cereb Cortex **22**, 2715-2732.

[87] Damoiseaux JS, Prater KE, Miller BL, Greicius M (2012) Functional connectivity tracks clinical deterioration in Alzheimer's disease. Neurobiol Aging **33**, 828.e19-30.

[88] Jones DT, Machulda MM, Vemuri P, McDade EM, Zeng G, Senjem ML, Gunter JL, Przybelski SA, Avula RT, Knopman DS, Boeve BF, Petersen RC, Jack CR Jr (2011) Age-related changes in the default mode network are more advanced in Alzheimer disease. Neurology **77**, 1524-1531.

[89] McGeown WJ, Shanks MF, Forbes-McKay KE, Venneri A (2009) Patterns of brain activity during a semantic task differentiate normal aging from early Alzheimer's disease. Psychiatry Res **173**, 218-227.

Tables

Table 1.

Statistical comparison of raw neuropsychological scores between the two diagnostic categories included in the study

Neuropsychological Test	Controls	Patients	p
Mini Mental State Examination	28.98 (1.37)	26.38 (3.01)	< 0.001
Raven's Progressive Matrices	29.78 (4.75)	26.11 (6.04)	0.002
Letter Fluency Test	34.16 (12.44)	29.80 (10.84)	0.080
Category Fluency Test	40.87 (10.35)	28.51 (8.95)	< 0.001
Digit Cancellation Test	53.11 (5.43)	46.11 (9.38)	< 0.001
WAIS - Similarities	20.58 (5.10)	18.00 (5.18)	0.019
Token Test	34.28 (1.95)	33.03 (2.86)	0.019
Rey-Osterrieth Complex Figure - Copy	32.24 (3.46)	28.91 (5.51)	0.001
Rey-Osterrieth Complex Figure - Recall	15.58 (5.81)	7.96 (4.82)	< 0.001
Stroop Test - Time Interference	24.28 (9.14)	38.40 (20.56)	< 0.001
Stroop Test - Error Interference	1.07 (2.95)	3.36 (6.01)	0.025
Digit Span - Forward	5.98 (0.99)	5.53 (0.84)	0.024
Visuospatial Span	4.78 (0.82)	4.07 (0.78)	< 0.001
Prose Memory – Total Recall	22.22 (7.97)	12.53 (8.07)	< 0.001
Paired Associated	13.07 (4.19)	8.67 (3.65)	< 0.001

Differences between the two groups were investigated with between-sample t tests

Table 2.

Statistical comparison of the four subgroups

Variable	Healthy Controls		AD Patients		p $_{Anova/\chi2}$	Post Hoc Significance
	1 - Low-Performing (n = 19)	2 - High-Performing (n = 26)	3 - Low-Performing (n = 23)	4 - High-Performing (n = 22)		
Demographics						
Education Level (years)	9.26 (4.71)	11.42 (4.45)	8.17 (4.22)	10.86 (4.05)	0.048 *	none
Age at Scan (days)	26312.42 (2023.80)	25687.00 (1793.946)	26551.17 (1372.07)	26816.27 (1785.36)	0.142	
Gender (male/female)	12/7	9/17	11/12	12/10	0.266	
Mini Mental State Examination	28.63 (1.64)	29.23 (1.11)	25.61 (3.39)	27.18 (2.363)	< 0.001 *	3 < 1, 2; 4 < 2
Neurostructural Index						
Gray-Matter Volume (cl)	591.80 (89.78)	567.56 (53.22)	527.81 (58.43)	540.12 (59.17)	0.009 *	3 < 1
White-Matter Volume (cl)	454.85 (42.57)	446.98 (57.33)	431.30 (54.20)	444.47 (70.56)	0.601	
Total Intracranial Volume (cl)	1685.56 (168.83)	1659.34 (164.41)	1673.54 (157.95)	1678.08 (246.56)	0.971	
Gray-Matter Fraction	0.35 (0.03)	0.34 (0.02)	0.32 (0.03)	0.33 (0.03)	< 0.001 *	3 < 1, 2; 4 < 1
White-Matter Fraction	0.27 (0.02)	0.27 (0.02)	0.26 (0.03)	0.27 (0.02)	0.175	
Brain Parenchymal Fraction	0.62 (0.04)	0.61 (0.03)	0.57 (0.04)	0.59 (0.04)	< 0.001 *	3 < 1, 2
Neuropsychological Scores						
Raven's Progressive Matrices	30.67 (4.32)	31.47 (3.39)	27.28 (5.03)	29.78 (5.14)	0.012 *	3 < 2
Letter Fluency Test	27.16 (6.97)	43.92 (7.07)	26.52 (6.64)	41.45 (7.08)	< 0.001 *	3 < 2, 4; 1 < 2, 4
Category Fluency Test	40.68 (6.25)	47.35 (9.26)	32.04 (6.34)	34.91 (10.52)	< 0.001 *	3 < 1, 2; 4 < 2
Digit Cancellation	52.49 (5.34)	53.39 (6.49)	43.27 (8.46)	49.80 (8.05)	< 0.001 *	3 < 1, 2, 4
Token Test	33.74 (1.72)	34.21 (2.11)	32.32 (3.03)	33.99 (1.87)	0.026 *	3 < 2
Rey-Osterrieth Complex Figure - Copy	33.78 (2.89)	33.10 (3.37)	29.75 (5.58)	30.97 (5.56)	0.014 *	3 < 1
Rey-Osterrieth Complex Figure - Recall	19.80 (5.28)	18.05 (5.31)	11.23 (5.29)	12.52 (4.45)	< 0.001 *	3 < 1, 2; 4 <1, 2
Stroop Test - Time Interference	16.09 (9.29)	15.22 (8.63)	35.79 (22.06)	20.59 (13.86)	< 0.001 *	3 > 1, 2, 4
Stroop Test - Error Interference	1.38 (3.89)	0.26 (0.71)	4.55 (7.48)	0.77 (1.95)	0.004 *	3 > 2, 4
Digit Span - Forward	6.00 (0.70)	6.04 (1.08)	5.66 (0.91)	5.76 (0.75)	0.410	
Visuospatial Span	5.07 (0.69)	4.99 (0.76)	4.40 (0.61)	4.41 (0.77)	0.001 *	3 < 1, 2; 4 <1, 2

Prose Memory - Total Recall	20.60 (7.41)	23.09 (7.01)	10.27 (6.83)	15.97 (7.78)	< 0.001 *	3 < 1, 2; 4 < 2
Paired Associated	13.70 (2.26)	13.59 (3.54)	9.16 (3.06)	11.29 (3.71)	< 0.001 *	3 < 1, 2

Differences among the four subgroups were tested with 1×4 ANOVAs. Differences in gender ratios were tested with a chi-squared test. The performance on neuropsychological measures included in the table was corrected for relevant demographic variables (age and education levels for all tests, with the addition of gender for the tests with a considerable visuospatial component) as indicated by normative guidelines [57, 58, 59, 60, 61, 62, 63]. The asterisk indicates a significant difference among the four sub-groups. Post-hoc test significance (Bonferroni corrected) is indicated in the column on the far right.

Table 3

Group differences in brain structure and network connectivity between the cohort of patients and the cohort of healthy controls

Cluster Number	Cluster Size (voxels)	Cluster-Level p_{FWE}	Z Score at Local Maximum	Side	Brain Region	BA	Talairach Coordinates		
							x	y	z
					Gray Matter: Controls > Patients				
1	24250	<0.001	5.96	L	Parahippocampal Gyrus	34	-12	-12	-16
			5.49	L	Middle Temporal Gyrus	22	-63	-35	4
			5.42	R	Middle Occipital Gyrus	18	12	-98	16
			5.42	R	Thalamus		6	-17	14
			5.38	L	Paracentral Lobule	31	-6	-19	47
			5.33	L	Superior Temporal Gyrus	22	-67	-38	11
			5.23	L	Middle Temporal Gyrus	21	-65	-36	-15
			5.22	L	Superior Parietal Lobule	7	-34	-49	60
			5.12	R	Middle Temporal Gyrus	19	57	-67	16
			5.09	L	Insula		-38	-19	6
			5.07	R	Paracentral Lobule	31	6	-11	47
			5.03	L	Supramarginal Gyrus	40	-59	-59	32
			5.02	L	Middle Temporal Gyrus	21	-59	-58	3
			5.01	L	Temporal Sub-Gyral	21	-42	-2	-8
			5.01	R	Middle Cingulate Gyrus	31	2	-31	40
			4.94	L	Insula		-40	-4	8
2	446	0.016	5.03	R	Postcentral Gyrus	5	30	-43	63
			4.20	R	Postcentral Gyrus	7	14	-53	65
			4.05	R	Superior Parietal Lobule	7	22	-59	60
3	5117	<0.001	4.61	R	Inferior Temporal Gyrus	20	36	-2	-44
			4.51	R	Superior Temporal Gyrus	22	53	4	0
			4.48	R	Temporal Sub-Gyral	21	44	-2	-8
4	373	0.032	4.57	L	Superior Frontal Gyrus	10	-18	66	6

			4.46	L	Superior Frontal Gyrus	10	-26	62	-11
			4.30	L	Middle Frontal Gyrus	10	-46	52	-6
5	1274	<0.001	4.28	R	Anterior Cingulate Gyrus	32	2	47	9
			4.08	R	Orbital Gyrus	11	6	42	-22
			4.02	L	Rectal Gyrus	11	-8	34	-24
6	357	0.037	4.15	R	Middle Frontal Gyrus	47	51	42	-7
			3.62	R	Inferior Frontal Gyrus	45	55	35	0
			3.58	R	Middle Frontal Gyrus	11	44	52	-14
				pDMN: Controls > Patients					
7	107	0.037	3.87	L	Middle Cingulate Gyrus	23	-2	-24	23
			3.83	R	Middle Cingulate Gyrus	23	6	-28	31
			3.14	R	Middle Cingulate Gyrus	31	6	-36	26
				rECN: Patients > Controls					
8	111	0.029	4.29	L	Superior Parietal Lobule	7	-34	-50	58
			4.10	L	Superior Parietal Lobule	7	-26	-53	63
				CBN: Patients > Controls					
9	128	0.017	4.16	R	Precentral Gyrus	4	59	-8	34
			4.01	R	Precentral Gyrus	6	50	-12	34
				OVN: Controls > Patients					
10	98	0.057	5.09	R	Caudate Head		12	23	-1
			3.30	R	Caudate Head		4	18	3

BA: Brodmann Area; L: Left; R: Right

Table 4.

Diagnosis-by-level of performance interaction in the pattern of resting-state network connectivity

Cluster Number	Cluster Size (voxels)	Cluster-Level p_{FWE}	Z Score at Local Maximum	Side	Brain Region	BA	Talairach Coordinates		
							x	y	z
				aDMN					
1	159	0.018	4.36	L	Cuneus	18	-4	-74	26
			3.98	R	Cuneus	18	4	-73	22
			3.59	R	Precuneus	31	-18	-71	18
				lECN					
2	294	0.001	4.88	L	Precuneus	31	-2	-74	26
			4.24	L	Precuneus	31	-10	-71	24
			3.77	L	Cuneus	19	-14	-84	34
3	255	0.002	4.23	L	Middle Temporal Gyrus	39	-38	-63	20
			4.09	L	Middle Temporal Gyrus	19	-42	-81	21
			3.97	L	Middle Temporal Gyrus	39	-38	-73	18
				rECN					
4	186	0.010	4.31	L	Cuneus	18	-18	-71	15
			4.00	L	Posterior Cingulate	30	-16	-62	9

Only significant findings are reported. BA: Brodmann Area; L: Left; R: Right

Table 5.

Post-hoc differences in network connectivity between high-performing and low-performing patients

Cluster Number	Cluster Size (voxels)	Cluster-Level p_{FWE}	Z Score at Local Maximum	Side	Brain Region	BA	Talairach Coordinates		
							x	y	z
aDMN - Increase: High-performing patients > Low-Performing patients									
1	185	0.008	4.46	L	Middle Temporal Gyrus	19	-44	-79	19
			4.02	L	Middle Occipital Gyrus	19	-28	-92	23
			3.56	L	Cuneus	19	-26	-82	24
lECN - Increase: High-performing patients > Low-Performing patients									
2	389	<0.001	4.53	L	Middle Temporal Gyrus	19	-44	-79	19
			4.00	L	Middle Occipital Gyrus	19	-30	-87	17
			3.99	L	Cuneus	19	-26	-80	24
3	291	0.001	4.24	L	Cuneus	18	-4	-76	26
			4.05	R	Cuneus	18	4	-75	22
			3.99	L	Cuneus	19	-12	-88	25
4	141	0.034	4.18	R	Middle Occipital Gyrus	18	24	-86	19
			3.29	R	Cuneus	18	18	-94	19
rECN - Increase: High-performing patients > Low-Performing patients									
5	186	0.008	5.08	L	Middle Temporal Gyrus	19	-44	-77	19
6	116	0.059	4.94	L	Middle Temporal Gyrus	21	-59	-39	0
			3.65	L	Middle Temporal Gyrus	22	-50	-37	2
7	229	0.003	4.64	R	Cuneus	18	2	-81	19
			3.90	R	Cuneus	30	10	-69	9

BA: Brodmann Area; L: Left; R: Right

Figure legends

Fig. 1

Overview of the multi-step procedure of extraction of dually-regressed maps of network functional connectivity. Z-score maps of the six components included in the study are depicted on the top right: in the column on the left, top down aDMN, pDMN and OVN; in the column on the right, top down: lECN, rECN and CBN. Slices in the Montreal National Institute space are as follows: aDMN: z = 24, x = -4; pDMN: z = 24, x = -4; OVN: z = 4, x = -4; lECN: z = 40, x = -40; rECN: z = 40, x = 40; CBN: z = -20, x = -4

Fig. 2

Effect of the group-by-performance interaction on the dually-regressed network maps. Slices in the Montreal National Institute space are as follows: aDMN: x = -4; z = 24; lECN: x = -5, z = 20, x = -40; rECN: x = -16, z = 12

Fig. 3

Post-hoc comparison between each sub-group of patient and the entire group of controls, testing group-differences between the values of functional connectivity within each of the clusters where a significant interaction effect was found. * = $p < 0.05$; ** = $p < 0.01$; *** = $p < 0.001$

Figure 1

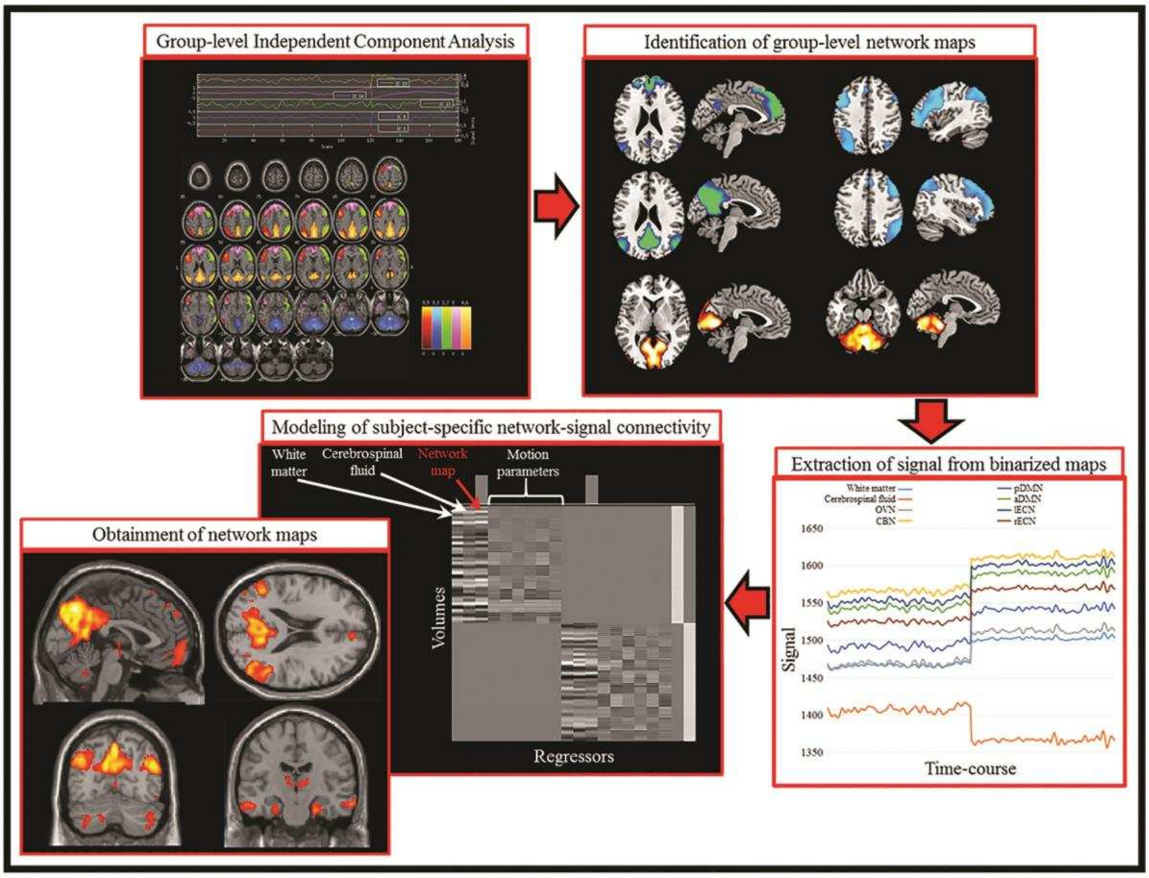
Group-level Independent Component Analysis
Identification of group-level network maps
Modeling of subject-specific network-signal connectivity
White matter
Cerebrospinal fluid
Network map
Motion parameters
Volumes
Regressors
Extraction of signal from binarized maps
White matter
Cerebrospinal fluid
OVN
CBN
pDMN
aDMN
lECN
rECN
Signal
Time-course
Obtainment of network maps

Figure 2

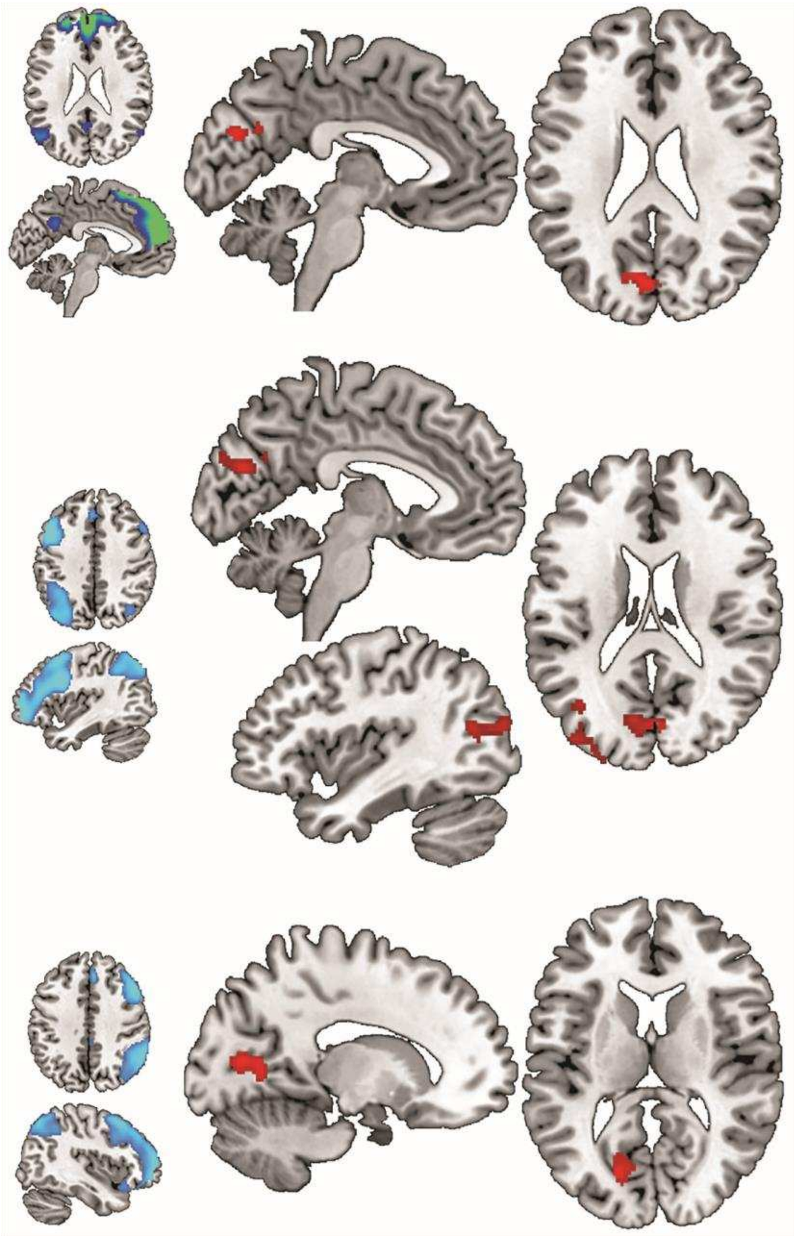

Figure 3

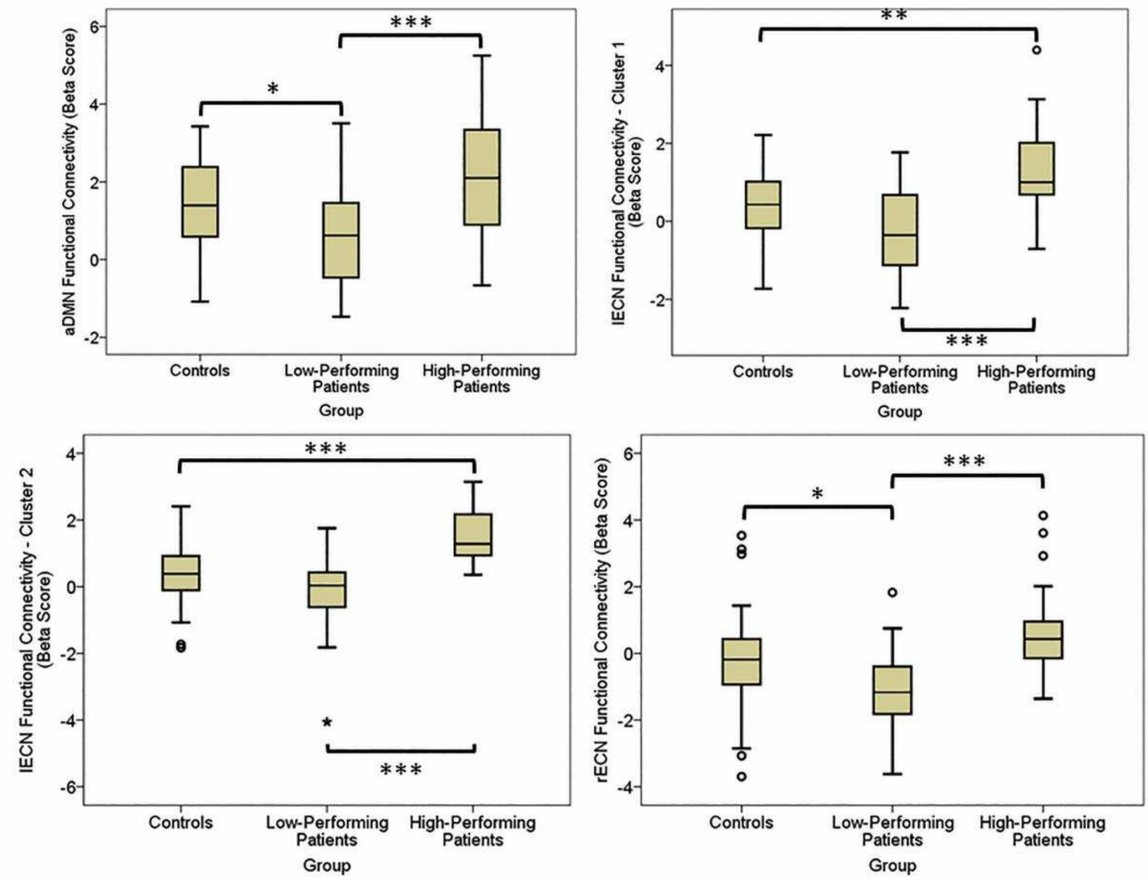

aDMN Functional Connectivity (Beta Score)
lECN Functional Connectivity - Cluster 1 (Beta Score)
lECN Functional Connectivity - Cluster 2 (Beta Score)
rECN Functional Connectivity (Beta Score)
Controls
Low-Performing Patients
High-Performing Patients
Group
*
**
***